Supplementary Information

Preparation of TiO_2-Supported Twinned Gold Nanoparticles by CO Treatment and Their CO Oxidation Activity

Junya Ohyama,[*,a,b] Taiki Koketsu,[a] Yuta Yamamoto,[c] Shigeo Arai,[c] Atsushi Satsuma[*,a,b]

[a] Graduate School of Engineering, Nagoya University, Nagoya 464-8603, Japan.

[b] Elements Strategy Initiative for Catalysts and Batteries (ESICB), Kyoto University, Katsura, Kyoto 615-8520, Japan.

[c] Ecotopia Science Institute, Nagoya University, Nagoya, 464-8603, Japan

Experimental

Materials. TiO_2 (JRC-TIO-8) was provided by the Catalysis Society of Japan. $HAuCl_4$ and NaOH were purchased from Kishida Chemical Co., Ltd.

Catalyst preparation. Au/TiO_2 was prepared by a precipitation deposition method. To a suspension of TiO_2 (0.297 g, after calcination at 400˚C under air for 3 h) in $HAuCl_4$ aq. (1.03 mM, 20 mL) was added NaOH aq. (0.10 M) to adjust the pH to 7.0 at room temperature. The suspension was warmed at 343 K under stirring for 1 h. The solid was separated by centrifugation and washed five times with 30 mL of distilled water. After the wash water was removed, the slurry was dried in a desiccator containing dry silica gel for 48 h at r.t.

Catalytic reaction. The as-prepared Au/TiO_2 (10 mg) in a fixed-bed flow reactor (a Pyrex glass tube) was treated under a flow of 4%CO/Ar with a flow rate of 10 mL min^{-1} for 30 min to prepare Au/TiO_2-CO. In the case of Au/TiO_2-H, the as-prepared Au/TiO_2 (10 mg) was treated under a H_2 flow (100%H_2) at 200˚C. For comparison, Au/TiO_2 was also treated under a gas flow consisting of H_2 (3%) and CO (0.4%) at 200 ˚C (Au/TiO_2-H+CO). After the treatments and following gas replacement with Ar, catalytic test was conducted in the reactor under a flow of 0.4%CO/10%O_2/Ar with a total flow rate of 100 mL min^{-1}. The reaction temperature was increased stepwise from r.t. to 100˚C. At each temperature, the steady state CO conversion was measured using nondispersive infrared (NDIR) CO/CO_2 analyzer (Horiba VIA510). The CO conversion was calculated by $CO_2/(CO+CO_2)$. The sum of CO and CO_2 concentration was constant during the reaction over all of the catalysts. The mass balance, (generated CO_2)/(converted CO), was 100%.

UV-vis spectroscopy. Diffuse reflectance UV-vis spectra were collected by a JASCO V-670 spectrometer equipped with an integral sphere. $BaSO_4$ was used as a standard reflection sample. The spectra were transformed with the Kubelka-Munk function.

STEM observation. STEM samples were prepared by depositing drops of methanol suspensions of the catalysts on carbon-coated Cu grids (Okenshoji Co. Ltd.). HAADF STEM images were obtained on a JEOL-ARM200F operated at 200 kV (magnification: 5 M with 2048 × 2048 pixels or at 10 M with 1024 × 1024 pixels (these give an identical length per pixel ratio)). The electron dose was ca. 1.0×10^4 e $Å^{-2}$.

XAFS spectroscopy. Au L_3 edge XAFS measurement was carried out on the BL01B1 beamline of SPring-8 with a Si(111) two-crystal monochromator (8 GeV, 100 mA). The XAFS spectra of the Au catalysts were recorded in fluorescence mode using a Lytle detector with a Ga filter. Data reduction

was performed using the program Athena ver. 0.9.21.included in the Demeter package.[1] The k^3 weighted EXAFS oscillation in the range of 3-11 $Å^{-1}$ was Fourier-transformed.

Inductively coupled plasma (ICP) spectroscopy. The loading of Au was determined by inductively coupled plasma spectroscopy using a Thermo IRIS Intrepid II (Thermo Electron Corp.).

Measurement of surface area. The specific surface areas of the samples before the reaction were determined by N_2 adsorption at liquid N_2 temperature using a conventional flow-type adsorption apparatus based on the Brunauer-Emmett-Teller (BET) method.

X-ray diffraction (XRD). XRD patterns of the samples before the reaction were recorded on a Rigaku MiniFlex II/AP diffractometer with Cu *K*α radiation.

X-ray photoelectron spectroscopy (XPS). The XPS of the samples before the reaction were obtained on a JPS-9000MC system (JEOL Ltd.) using Al *K*α radiation. The energy was corrected by referencing the C1s peak to 285.0 eV.

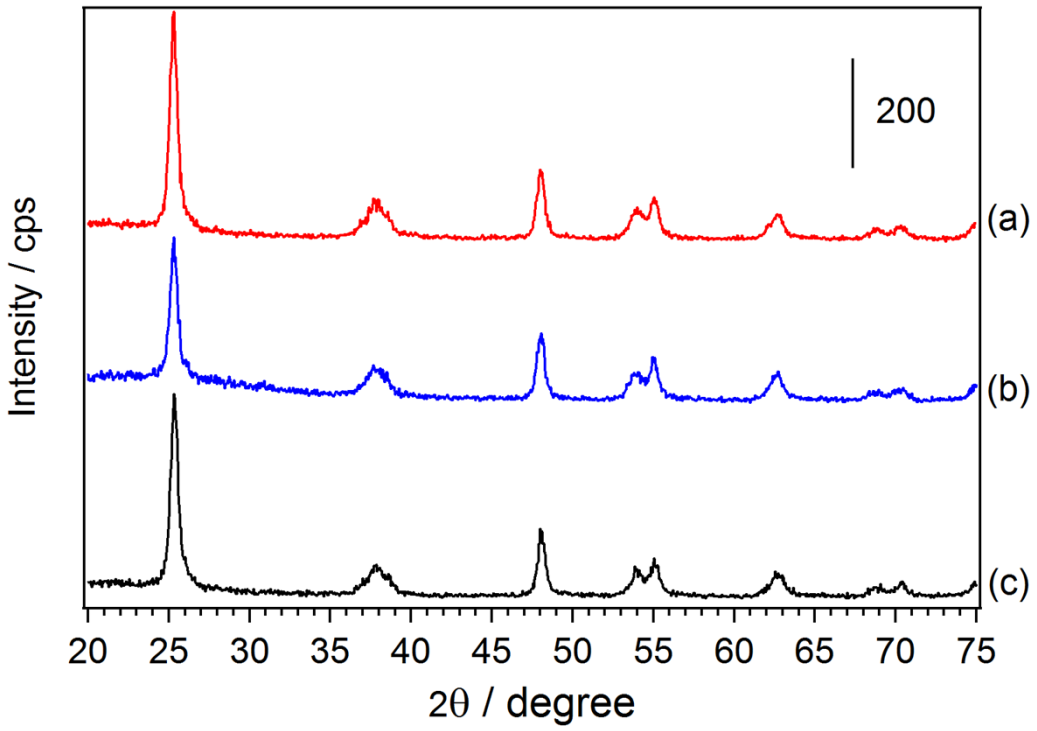

Fig. S1. XRD patterns of (a) Au/TiO_2-CO, (b) Au/TiO_2-H, and (c) TiO_2. All of the samples showed an identical pattern of TiO_2 with anatase phase.

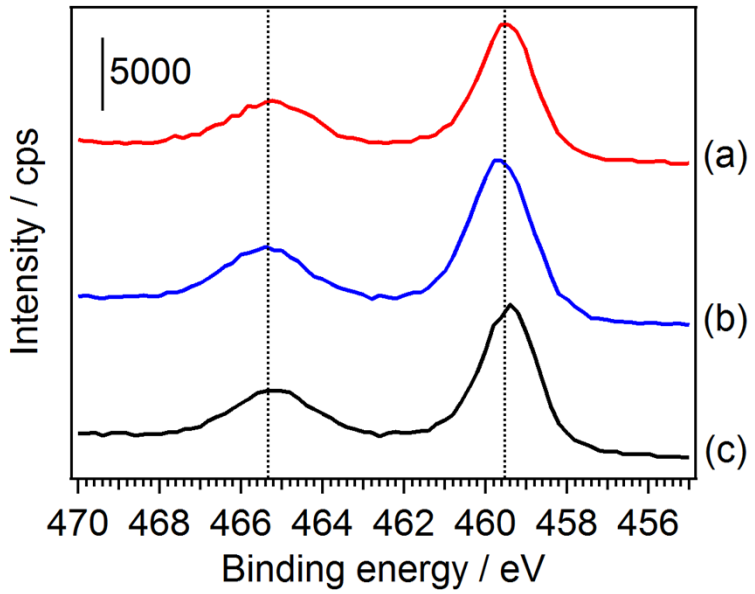

Fig. S2. Ti 2p XPS of (a) Au/TiO_2-CO, (b) Au/TiO_2-H, and (c) TiO_2 (JRC-TIO8 after calcination at 400˚C without Au) as a reference. The energies of Ti 2p peaks did not change by the deposition of AuNPs on TiO_2. Therefore, the surface chemical state of TiO_2 showed little change by the preparation.

EXAFS analysis

The Au L_3 edge EXAFS spectra were analyzed to obtain structural parameters as shown in Table S1. The atomic distance of Au-Au (r) of Au/TiO_2-CO was larger than Au/TiO_2-H_2. The large r of Au/TiO_2-CO might be due to multiple twinned structures as well as due to the larger size of AuNPs. Au/TiO_2-CO also showed the larger coordination number of Au-Au (CN) compared with Au/TiO_2-H, indicating the larger AuNPs of Au/TiO_2-CO than those of Au/TiO_2-H. The result is consistent with the STEM analysis (Fig.).

Table S1. Structural parameters determined by the curve fitting analysis of the Au L_3 edge EXAFS spectra of Au/TiO_2-CO and Au/TiO_2-H.[a]

Catalyst	r [b] / Å	CN [c]	DW [d] / $Å^{-2}$	R factor [e]
Au/TiO_2-CO	2.816(7)	3.2(4)	0.011(1)	0.00418
Au/TiO_2-H_2	2.721(7)	1.6(2)	0.009(1)	0.00504

[a] Curve fitting range: k = 3-11 $Å^{-1}$, r = 2.0-3.3 Å. [b] Atomic distance of Au-Au. [c] Coordination number of Au-Au. [d] Debye-Wallaer factor. [f] R factor.

Another TiO_2 supported AuNPs

A JRC-TIO4 (equivalent to P25) supported Au catalyst was prepared by the same procedure as above, and treated by CO at r.t. (Au/JRC-TIO4-CO) and H_2 at 200˚C (Au/JRC-TIO4-H). By using the catalysts, the CO oxidation was conducted at r.t. The CO conversion over Au/JRC-TIO4-CO (95%) was higher than that of Au/JRC-TIO4-H (78%). Therefore, as is the case with JRC-TIO-8, the CO reduction treatment at r.t. enhanced the CO oxidation activity compared to the H_2 reduction at 200˚C.

Treatment of Au/TiO_2 under a mixed gas of H_2 and CO

The effect of CO as a reductant was further investigated by using Au/TiO_2 treated under a mixed gas of H_2 and CO at 200˚C (Au/TiO_2-H+CO). Au/TiO_2-H+CO showed higher catalytic activity for CO oxidation at r.t. (CO conversion of 76%) compared with Au/TiO_2-H (CO conversion of 37%). It is possible that CO leads the formation of twinned AuNPs to enhance the catalytic activity.

Comparison of the Turnover frequency (TOF) with the previous literatures

To calculate the TOF on Au/TiO_2-CO, the CO oxidation reaction was carried out at 3˚C, because the CO conversion at r.t. is ca. 80%, where the diffusion limitation of the reactant (CO) largely

contributes the reaction rate. The CO conversion over Au/TiO_2-CO at 3˚C was 50%. Table S2 lists the TOFs of Au/TiO_2-CO at 3˚C together with the TOFs of Au/TiO_2 catalysts in the literatures.[2-4] The TOF was higher than those reported previously. It is suggested that the CO treatment is effective to enhance the CO oxidation activity in comparison with the conventional treatment methods.

Table S2. TOF of CO oxidation over Au/TiO_2-CO together with the TOFs of Au/TiO_2 in the literatures.[2-4]

TOF	Reaction temperature (˚C)	Ref.
0.58 [a]	3	This study
< 0.15	0	*J. Catal.* **1993**, *144*, 175.
<0.16	5	*J. Catal.* **2004**, *222*, 357.
< 0.06	0	*J. Catal.* **2006**, *241*, 56.

[a] The TOF (number of CO molecules converted per number of surface atom of AuNPs per second) was calculated on the assumption of hemispherical structure of AuNPs.

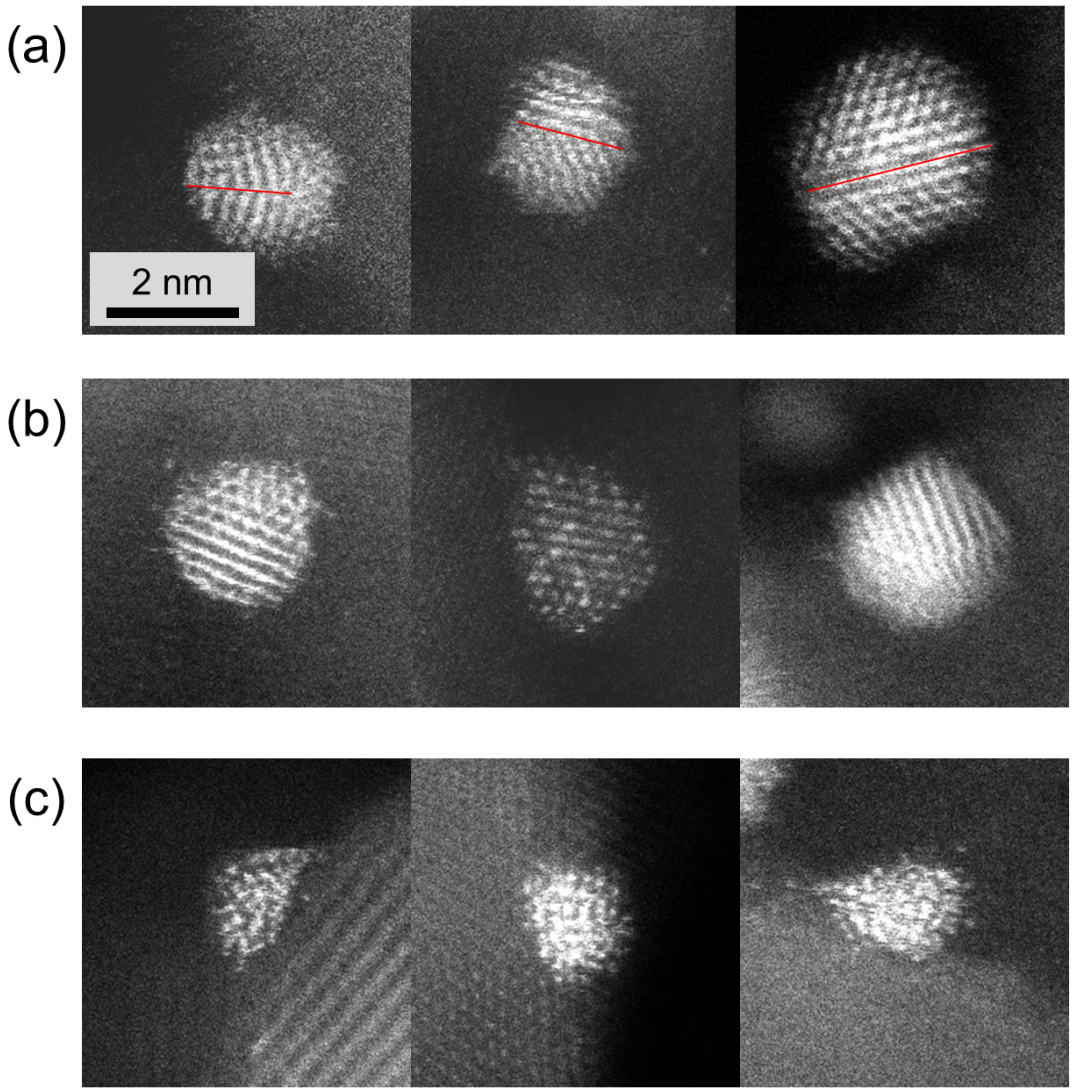

Fig. S3. Atomic resolution HAADF STEM images of (a) T-AuNPs, (b) S-AuNPs, and (c) A/U-AuNPs. The red lines on (a) indicates apparent twin boundaries.

Stability of Au/TiO_2-CO

The CO oxidation reaction over Au/TiO_2-CO was carried out at r.t. for 10 h as shown in Fig. S4. The CO conversion decreased fast in early times (by 4% at 0.5 h), and then slowly (by 9% at 10 h). On the other hand, the STEM analysis of Au/TiO_2-CO after 0.5 h did not show significant changes in the particle size by the reaction (Figs. 3 and S5) and the crystal structure of AuNPs (Fig. S6). The feature of the time course of the CO conversion (Fig. S4) was similar to the literature.[5] The decrease in the CO conversion might be due to the surface carbonate formation on the catalyst, rather than the change in the structure of AuNPs.[5]

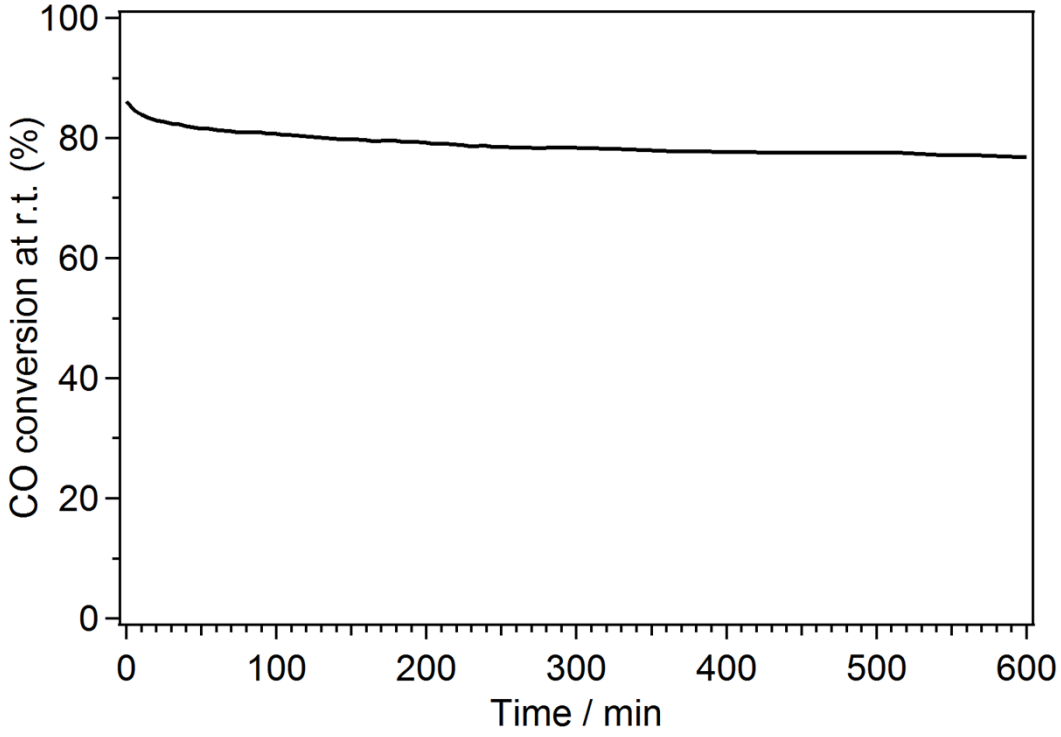

Fig. S4. Time course of the CO conversion on Au/TiO_2-CO for 10 h.

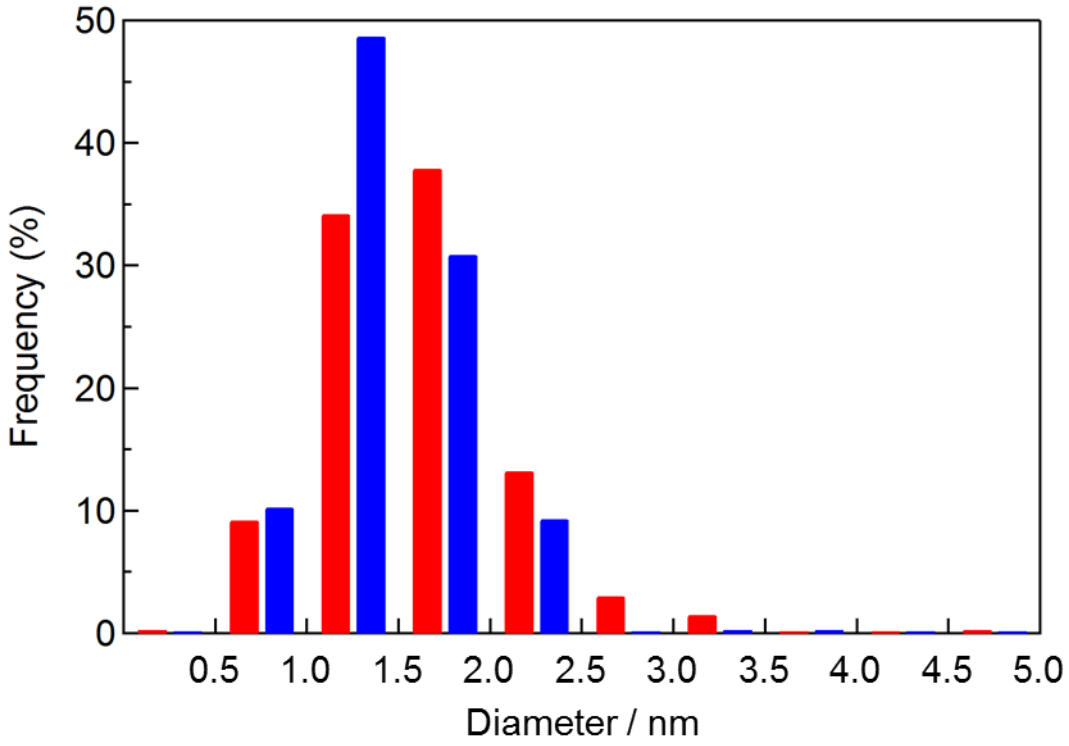

Fig. S5. The particle size distributions of Au/TiO_2-CO and Au/TiO_2-H before the CO oxidation reaction. The average particle sizes of Au/TiO_2-CO and Au/TiO_2-H were 1.6 ± 0.5 nm and 1.5 ± 0.4 nm, respectively. The sizes did not change after the reaction for 0.5 h (1.6 ± 0.6 nm and 1.5 ± 0.4 nm for Au/TiO_2-CO and Au/TiO_2-H, respectively).

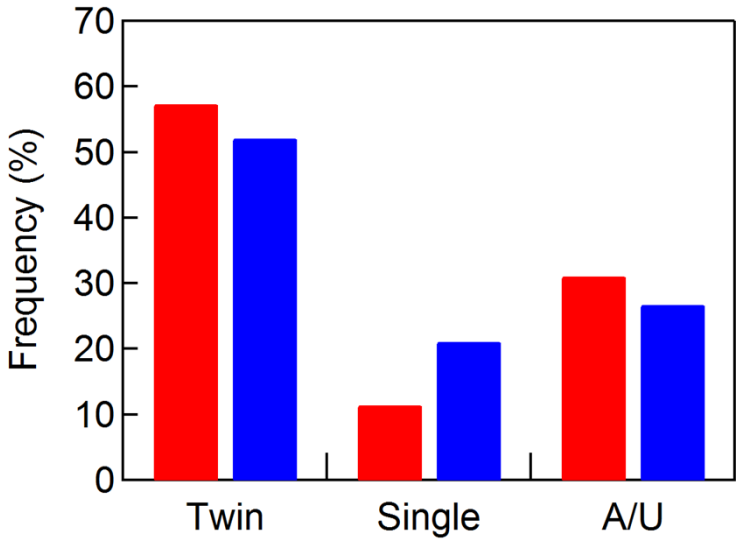

Fig. S6. Comparison of the crystal structure distributions of Au/TiO_2-CO before (red) and after (blue) the CO oxidation reaction for 0.5 h.

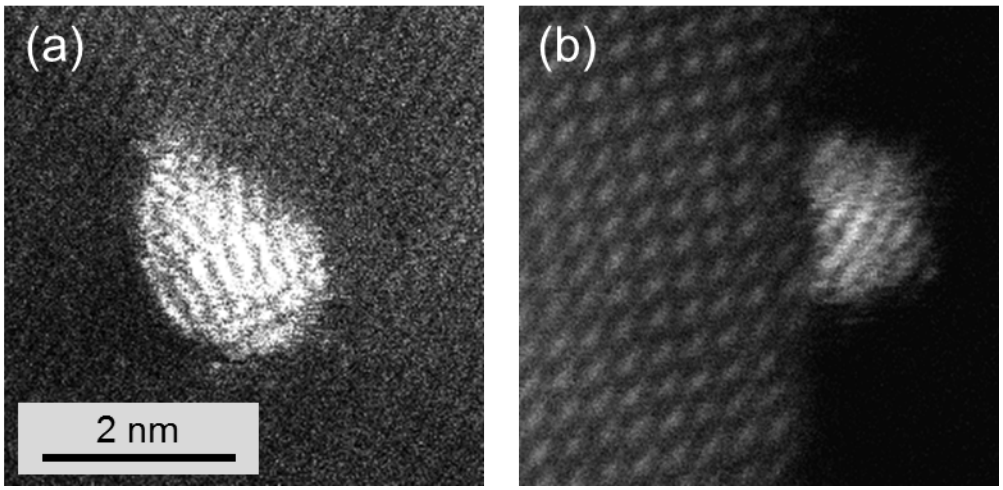

Fig. S7. HAADF STEM images showing half-cut (hemispherical-like) structure of AuNPs of (a) Au/TiO_2-CO and (b) Au/TiO_2-H.

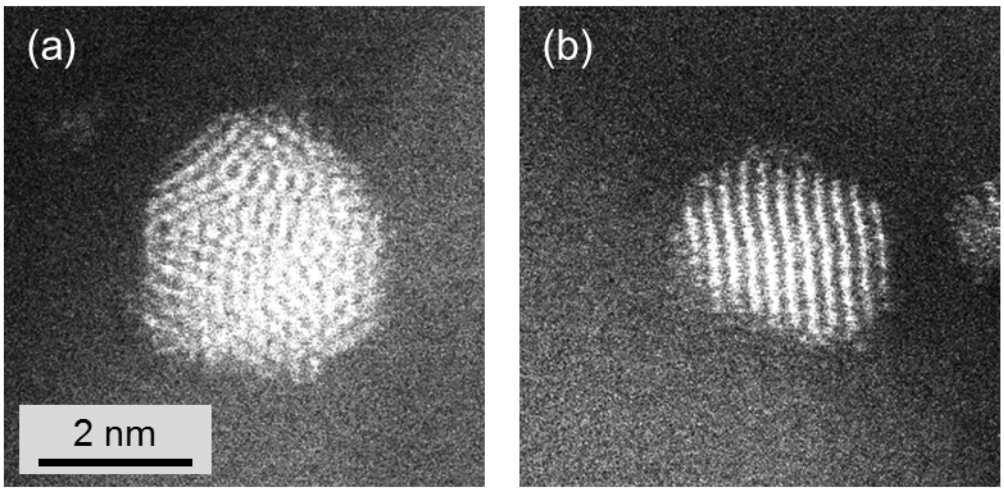

Fig. S8. HAADF STEM images of AuNPs showing facetted structures on (a) Au/TiO_2-CO and (b) Au/TiO_2-H.

Effect of residual water on CO oxidation reaction

It is well known that water on supported Au catalysts can enhance their catalytic activity.[6, 7] One might consider that the higher catalytic activity of Au/TiO_2-CO than Au/TiO_2-H is due to the residual water on Au/TiO_2-CO. Therefore, we immersed Au/TiO_2-H in water, and then dried in a desiccator containing dry silica gel for 48 h. By using the resulting sample (Au/TiO_2-HW), the catalytic test was conducted. However, the activity was not improved as shown in Fig. S9. The result suggests that the enhanced catalytic activity of Au/TiO_2-CO is not due to the residual water.

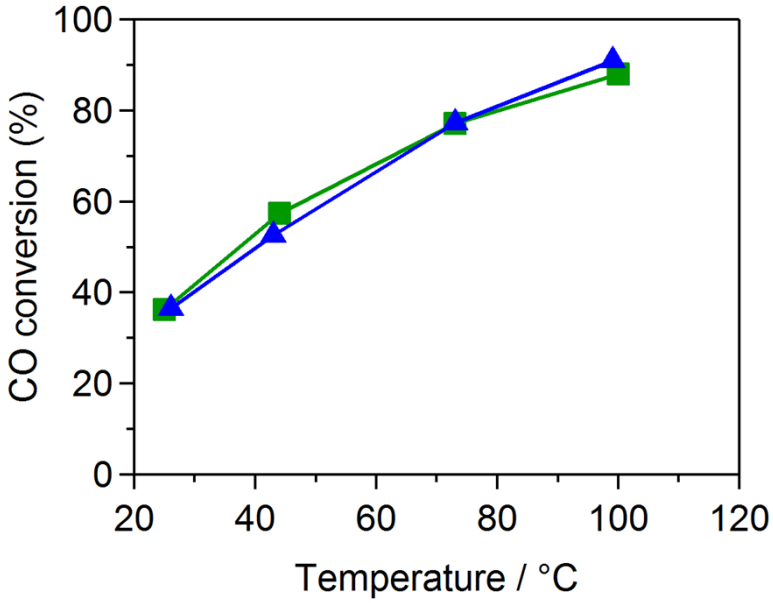

Fig. S9. CO conversion over Au/TiO_2-HW (green) and Au/TiO_2-H (blue).

References.

1. Ravel, B; Newville, M., J. *Synchrotron Rad.*, 2005, 12, 537

2. M. Haruta, S. Tsubota, T. Kobayashi, H. Kageyama, M.J. Genet, B. Delmon, *J. Catal.*, 1993, 144, 175.

3. R. Zanella, S. Giorgio, C.H. Shin, C.R. Henry, C. Louis, *J. Catal.*, 2004, 222, 357.

4. S.H. Overbury, V. Schwartz, D.R. Mullins, W. Yan, S. Dai, *J. Catal.*, 2006, 241, 56.

5. Y. Denkwits, M. Makosh, J. Geserick, U. Hörmann, S. Selve, U. Kaiser, N. Hüsing, R.J. Behm, *Appl Catal B*, 2009, 91 470.

6. T. Fujitani and I. Nakamura, *Angew. Chem. Int. Ed.*, 2011, 50, 10144.

7. T. Takei, T. Akita, I. Nakamura, T. Fujitani, M. Okumura, K. Okazaki, J. Huang, T. Ishida, M. Haruta, C. G. Bruce and C. J. Friederike, *Adv. Catal.*, 2012, 55, 1.